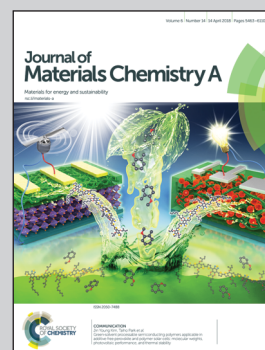Showcasing a study on the fabrication of the first highly sensitive MOF-based sensor for detection of sulfur dioxide (SO$_2$). The successful fabrication and investigation of the sensor based on a MOF thin film of MFM-300 (In) on an IDE capacitive electrode was accomplished by Prof. M. Eddaoudi's and Prof. K. N. Salama's groups at King Abdullah University of Science and Technology (KAUST) in Saudi Arabia.

Highly sensitive and selective SO$_2$ MOF sensor: the integration of MFM-300 MOF as a sensitive layer on a capacitive interdigitated electrode

Advantageously, porous MOFs offer great potential as a sensitive material, allowing selective adsorption and pre-concentration of the analytes. The sensor prepared in this study, based on a highly selective MOF material, revealed remarkable SO$_2$ sensitivity down to 75 ppb with excellent stability and selectivity to other common gases/vapors.

As featured in:

Journal of Materials Chemistry A

ROYAL SOCIETY OF CHEMISTRY

rsc.li/materials-a

COMMUNICATION

Check for updates

Highly sensitive and selective SO₂ MOF sensor: the integration of MFM-300 MOF as a sensitive layer on a capacitive interdigitated electrode†

Valeriya Chernikova,[a] Omar Yassine,[b] Osama Shekhah, [ID][a] Mohamed Eddaoudi [ID] *[a] and Khaled N. Salama [ID] *[b]

We report on the fabrication of an advanced chemical capacitive sensor for the detection of sulfur dioxide (SO₂) at room temperature. The sensing layer based on an indium metal–organic framework (MOF), namely MFM-300, is coated solvothermally on a functionalized capacitive interdigitated electrode. The fabricated sensor exhibits significant detection sensitivity to SO₂ at concentrations down to 75 ppb, with the lower detection limit estimated to be around 5 ppb. The MFM-300 MOF sensor demonstrates highly desirable detection selectivity towards SO₂ *vs.* CH₄, CO₂, NO₂ and H₂, as well as an outstanding SO₂ sensing stability.

Sulfur dioxide (SO₂) is regarded as one of the most toxic and problematic anthropogenic air pollutants.[1] Despite the fact that the world is becoming more receptive to the use of renewable energy alternatives, demand for fossil fuel is ever increasing. Notably, burning of fossil fuels by power plants entails a rise in SO₂ emission, posing a serious threat to the environment and human health.[2,3] It is to be noted that major health concerns are associated with prolonged exposure to SO₂, with a primary one-hour acceptable limit set at 75 parts per billion (ppb).[4] Certainly, it is necessary to continuously monitor the concentration of SO₂ in ambient air, particularly near emission sources.

Many studies have investigated compact SO₂ sensors based on different classes of gas-sensing materials, such as solid electrolytes,[5] conducting polymers,[6,7] metal oxide semiconductors,[8,9] and piezoelectric crystals,[10] which are applied on a variety of transduction units. Metal oxide semiconductors operate on a change of resistance when a targeted analyte reacts

[a]Functional Materials Design, Discovery and Development Research Group (FMD³), Advanced Membranes & Porous Materials Center, Division of Physical Sciences and Engineering, King Abdullah University of Science and Technology(KAUST), Thuwal 23955-6900, Kingdom of Saudi Arabia. E-mail: mohamed.eddaoudi@kaust.edu.sa

[b]Sensors Lab, Electrical Engineering Program, Computer, Electrical and Mathematical Science and Engineering Division, King Abdullah University of Science and Technology (KAUST), Thuwal 23955-6900, Kingdom of Saudi Arabia. E-mail: khaled.salama@kaust.edu.sa

† Electronic supplementary information (ESI) available. See DOI: 10.1039/c7ta10538j

with the chemisorbed oxygen from air.[11] These semiconductors are among the most promising candidates due to their low cost, high sensitivity, and reliability.[8,9] Device response and sensitivity are greatly influenced by the exposed surface area and operating temperatures, regulating the amount of oxygen adsorption and the formation of surface ionic species needed for the reaction with the analyte. Nevertheless, these sensors suffer from evident disadvantages such as high-power consumption and complex electrical system design. Manifestly, advanced preparation[8] and modification methods[12,13] are constantly enhancing the sensing performance of metal oxide sensors. For example, the coating of porous materials, such as zeolites, is used to pre-concentrate targeted gases and to avoid interference from the cross-sensitivity of larger non-targeted gases.[13] Despite the aforementioned progress, the quest for room-temperature stable and sensitive gas sensors has inspired researchers to consider alternative materials. For instance, reversible physisorption within porous materials with highly accessible pore systems prompting effective and selective interactions with analytes offers great potential for targeted gas sensing.[14]

Metal–organic frameworks (MOFs) are crystalline porous materials based on self-assembled metal ions or metal clusters with organic ligands into a periodic networked structure. Uniquely, MOF chemistry offers a myriad of tunable porous structures with unparalleled surface areas and tailor-made pore shapes, sizes and functionalities.[15,16] Prominently, various MOFs have shown high capacity and selectivity for harmful gases,[17] positioning MOFs as prospective candidates for gas-sensing applications.[14,18–23] Nevertheless, our previous work revealed that regulating the MOF pore size and shape is not sufficient to achieve the requisite effective detection of hazardous gases/vapors, and a more specific interaction/affinity between the targeted harmful adsorbates and the host framework is commanded.[24,25] Accordingly, we opted to select a MOF with predefined requisites, namely a high SO₂ uptake with the ability to congruently discriminate one gas over another and thus maximizing the potential selectivity towards the targeted

This journal is © The Royal Society of Chemistry 2018

analyte. A MOF encompassing the aforementioned criteria is prone to offer improved sensor performance in terms of response and selectivity. Although a substantial number of MOFs have been studied for potential SO_2 sorption,[26–31] to the best of our knowledge, no MOF-based SO_2 sensors have been reported so far. MOFs have not been applied for SO_2 detection, probably since the majority, and particularly those with open metal sites, are not stable upon exposure to SO_2.[32] The recently introduced indium based MFM-300 (In) MOF[26] was chosen among others such as MFM-300 (Al),[24] MFM-202-a,[28] $M_3[Co(CN)_6]_2$ (M = Zn, Co),[29] Mg–MOF-74,[30] and $Ni(bdc)(ted)_{0.5}$,[31] due to its high SO_2 sorption capacity of 8.28 mmol g^{-1} (298 K and 1 bar), and compatible (mild) synthetic conditions with sensor circuit stability during thin film deposition (Table S1†). MFM-300 (In) MOF is a 3-periodic open framework, isostructural to its aluminum[27] and gallium[33] analogues, and comprises infinite *cis* $InO_4(OH)_2$ octahedral chains bridged by tetradentate ligands (biphenyl-3,3′,5,5′-tetracarboxylic acid) (Fig. 1). Structural analysis of MFM-300 revealed the decoration of the pore system with OH- groups along the metal chains in the helical direction, thereby creating a periodic array of exposed free OH- groups in the surface of the pores. Markedly, the exposed OH- groups along with four neighbouring C–H groups from benzene rings provide "pocket-like" adsorption sites suitable for SO_2 binding, governing its adsorption selectivity toward SO_2 (Fig. S1†).[26]

One of the challenges in integrating MOFs into devices for various related applications is directly related to the ability to fabricate and deploy MOFs as thin films. Delightfully, recent advances have permitted the successful control of MOF thin film growth or deposition on various supports, including surface modification of substrates with self-assembled monolayers (SAMs) which we have used in the present study.[34–37] To evaluate the sensing properties of MFM-300 (In), a MOF thin film was coated on interdigitated electrodes (IDEs) and associated changes in capacitance were directly measured as a response to the presence of a given analyte.[24,25,38] Particularly,

the MFM-300 (In) MOF was grown on a prefunctionalized IDE with an OH-terminated SAM,[39–41] using an optimized solvothermal synthetic procedure[26] (Fig. 1). The successful fabrication of a highly crystalline, suitably intergrown crystals, and homogeneous MFM-300 (In) MOF thin film was confirmed using X-ray diffraction (XRD) and scanning electron microscopy (SEM) (Fig. 2, S2†).

The gas-sensing tests were performed using the established procedure reported previously,[24,25,42] where the samples were first activated under vacuum for one hour, and the chamber was later purged with pure nitrogen. Nitrogen gas was used as a carrier gas to dilute SO_2 (and other gases) to the desired concentration (*i.e.* down the ppb range).

The MFM-300 (In) MOF sensor performance was found to be exceptional as we were able to detect SO_2 in the ppb range down to 75 ppb with a linear response from 75 to 1000 ppb (Fig. 3a and b) with a detection limit as low as 5 ppb. The remarkable detection is plausibly governed by the associated changes in film permittivity upon adsorption of SO_2 molecules. Reasonably, two types of interactions regulated the adsorption process:[24] (i) analyte–framework interaction, in which oxygen centers from SO_2 ($O^{\delta-}$) form hydrogen bonds with the exposed hydrogen ($H^{\delta+}$) centers from free hydroxyl groups and four aromatic C–H groups from the ligand respectively; and (ii) analyte–analyte interaction, in which adsorbed SO_2 interacts with another SO_2 through dipoles. These electrostatic changes in the film are reflected in the observed change of capacitance.

These very promising results prompted us to evaluate the stability of the MFM-300 (In) MOF capacitive sensor for SO_2 detection at room temperature using reproducibility tests. In these tests, we explored the performance of the sensor in detecting two concentrations of SO_2, 500 and 1000 ppb, over a testing period of more than three weeks (Fig. 3c). The results clearly showed that the detection levels were steady/stable with
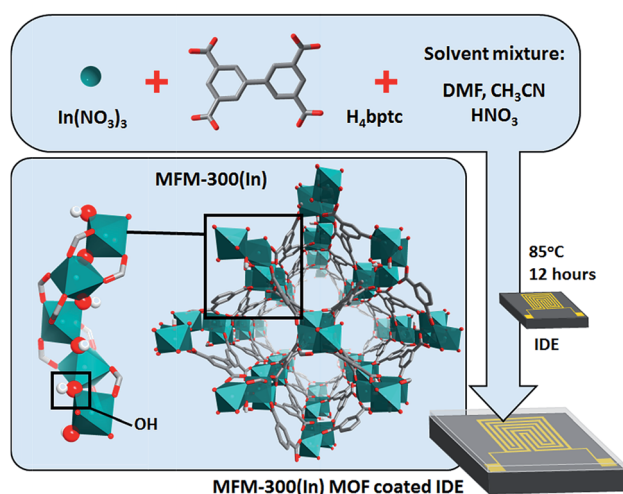

Fig. 1 Schematic representation of the optimized solvothermal preparation approach of MFM-300 (In) MOF thin film on the interdigitated electrodes (IDEs).
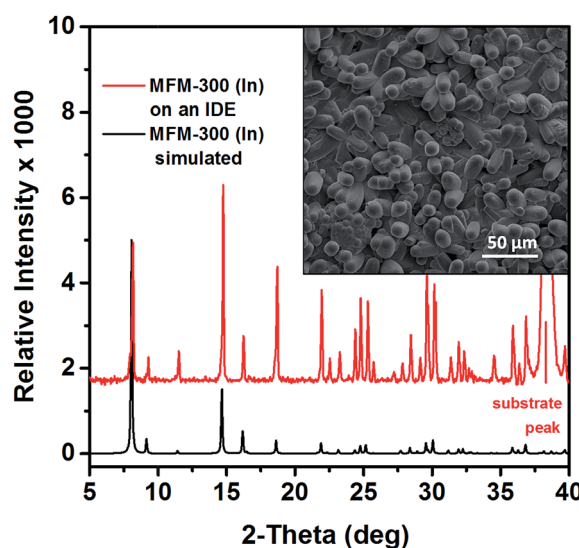

Fig. 2 Comparison of calculated X-ray diffraction (XRD) patterns of MFM-300–MOF (In) and thin film grown on the IDE. Top view SEM image of MFM-300–MOF (In) coating.
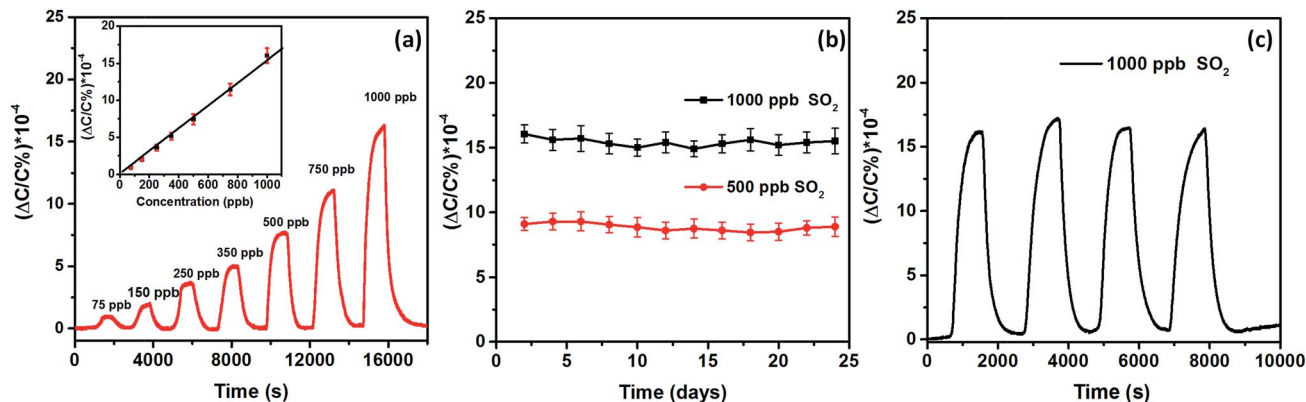
This journal is © The Royal Society of Chemistry 2018

J. Mater. Chem. A, 2018, **6**, 5550–5554 | **5551**

Fig. 3 (a) Detection of SO_2 in the 75 to 1000 ppb concentration range, insets: linear response for the corresponding range; (b) linear response for MFM-300 (In) MOF-based sensor upon exposure to 500 and 1000 ppb of SO_2 over a 24 day period; (c) reproducibility cycles for the detection of 1000 ppb of SO_2.

a negligible variation over the range of the tested period of time, attesting to the stability and durability of our SO_2 sensor over the range of tested concentrations.[42]

Subsequently, the effect of relative humidity (RH) on the performance of the MOF sensor was also investigated. The humidity in the chamber was adjusted to the desired level (5–85% RH) and capacitance response was subtracted as a baseline (Fig. S6 and 7†). The capacitance change was recorded at each RH level in the presence of SO_2 at 350 and 1000 ppb. Noticeably, distinctive signals for both SO_2 concentrations (Fig. 4a), similar to "dry" conditions (Fig. 3a), confirm the strong affinity of the MFM-300 (In) MOF sensor toward SO_2 and attest to its practical applicability in the presence of water molecules. The noted sensor performance under humid conditions suggests the possibility of competitive adsorption on hydroxyl groups between water and SO_2 at low humidity levels, and therefore, negligible change is observed up to 30% RH.[43] At higher humidity levels, adsorbed water in the MOF can increase sorption uptake of the analyte with water compared to the sorption uptake of the same analyte adsorbed on the dry framework, and, thus, increases the effect on capacitance

change. With the increase of humidity, the SO_2 interacts with adsorbed water by forming additional hydrogen bond interactions.[42,43]

The temperature (T) dependence of SO_2 sensitivity for the MFM-300 (In) MOF sensor was also evaluated in the range of 22–100 °C (Fig. 4b). The sensitivity response logically decreases with the temperature increase, because, in MFM-300 (In) MOF, as in most compounds, equilibrium sorption decreases with increasing temperature. The best sensitivity was obtained at 22 °C. Further, upon increasing the T from 22 °C to 80 °C, we observed a drop by almost 35%, which can be attributed to the lessened interactions toward exposed active sites, resulting in increased molecular diffusion and a decrease in the analyte adsorbed amount.

Finally, we investigated the selectivity of our MFM-300 (In) MOF sensor in the presence of various gases/vapors, including methane (CH_4), hydrogen (H_2), carbon dioxide (CO_2), nitrogen dioxide (NO_2), propane (C_3H_8) and toluene (C_7H_8) at 1000 ppb level (Fig. 4c). The response of the MFM-300 (In) MOF films to these gases was recorded using the same testing protocol, and the study revealed an excellent selectivity for SO_2 compared to
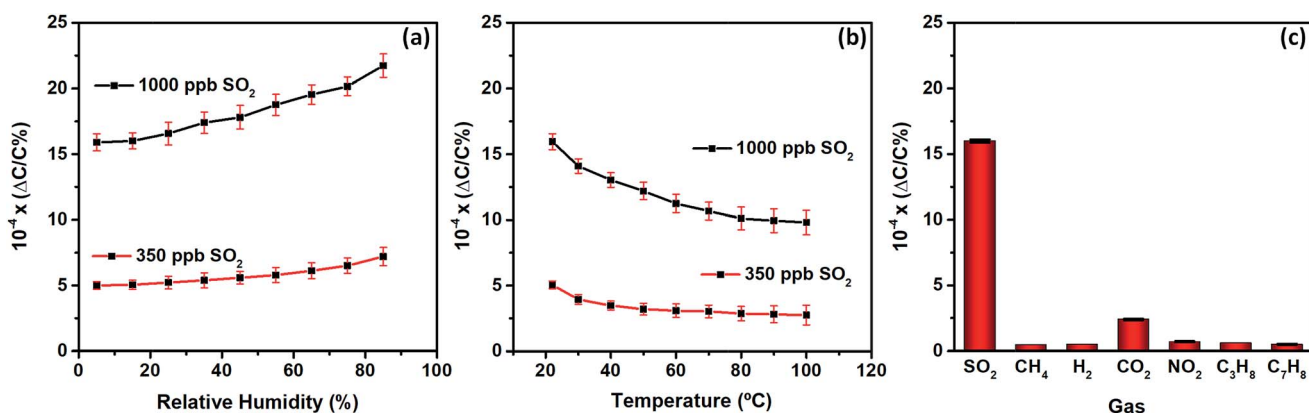

Fig. 4 Effects of the (a) relative humidity and (b) temperature on the MFM-300 (In) MOF sensor performance. (c) Selectivity of the MFM-300 (In) MOF sensor to other gases at 1000 ppb.

5552 | J. Mater. Chem. A, 2018, 6, 5550–5554

This journal is © The Royal Society of Chemistry 2018

the other gases/vapors, with slight cross-sensitivity with CO_2. However, the response signal of the MFM-300 (In) MOF to SO_2 was almost four times higher than for CO_2 and more than 20 times higher than other gases/vapors, which clearly corroborate the exceptional sensing selectivity of the MFM-300 (In) MOF sensor towards SO_2.

Table 1 presents a comparison of the performance of our MFM-300 (In) MOF-based capacitor sensor with selected benchmark material-based sensors. Currently, more than 90% of all reported material-based sensors for toxic gases represent a combination of two or more different types of materials, namely composites.[50–53] For example, a metal oxide/polymer composite allows SO_2 detection at room temperature, while a metal oxide on its own requires heating. In contrast, here we have presented for the first time a pure MOF-based SO_2 sensor that shows similar/improved performance compared to the best-reported sensors so far. Prominently for our unveiled SO_2 MOF sensor, the high affinity for SO_2 of the deposited MOF material, combined with the cheap and easy capacitive measurement, led to the attained superior SO_2 sensing performances. Therefore, in the future, the combination of this MOF with other advanced materials could offer great opportunities for the design of better performing sensors based on capacitance or other transduction mechanisms.

In conclusion, this study attests to the excellent performance and stability of the first MOF-based SO_2 sensor and its superior detection limit, which is considered to be the lowest reported sensitivity by an order of magnitude, in comparison to other sensors at room temperature. Principally, MFM-300 (In) MOF offers a distinctive SO_2 detection at concentrations down to 75 ppb with a limit of detection down to 5 ppb. The exceptional stability of the MFM-300 (In) MOF sensor was supported and demonstrated using reproducibility tests. Moreover, the presented results attest to the distinctive and remarkable sensing selectivity of the prepared MOF sensor towards SO_2, as shown

from the signal intensity associated with the MFM-300 (In) MOF for SO_2 detection compared to the associated signal intensities for other evaluated gases/vapors like NO_2, CH_4, H_2 and others. This unique sensing feature of the MFM-300 (In) MOF paves the way for the deployment of MOF-based sensors in various key sensing applications.

Conflicts of interest

There are no conflicts to declare.

Acknowledgements

Notes and references

1 J. N. Galloway, *Water, Air, Soil Pollut.*, 1995, **85**, 15–24.
2 M. Kampa and E. Castanas, *Environ. Pollut.*, 2008, **151**, 362–367.
3 P. L. Ward, *Thin Solid Films*, 2009, **517**, 3188–3203.
4 United States Environmental Protection Agency, NAAQS Table, https://www.epa.gov/criteria-air-pollutants/naaqs-table#4, accessed October, 2017.
5 J. W. Fergus, *Sens. Actuators, B*, 2008, **134**, 1034–1041.
6 A. J. Heeger, *Chem. Soc. Rev.*, 2010, **39**, 2354–2371.
7 V. Chaudhary and A. Kaur, *Polym. Int.*, 2015, **64**, 1475–1481.
8 G. F. Fine, L. M. Cavanagh, A. Afonja and R. Binions, *Sensors*, 2010, **10**, 5469–5502.
9 K. Wetchakun, T. Samerjai, N. Tamaekong, C. Liewhiran, C. Siriwong, V. Kruefu, A. Wisitsoraat, A. Tuantranont and S. Phanichphant, *Sens. Actuators, B*, 2011, **160**, 580–591.
10 O. M. Guimaraes, *Anal. Lett.*, 1997, **30**, 2159–2174.
11 T. Alammar, O. Shekhah, J. Wohlgemuth and A.-V. Mudring, *J. Mater. Chem.*, 2012, **22**, 18252–18260.
12 P. Tyagi, S. Sharma, M. Tomar, F. Singh and V. Gupta, *Nucl. Instrum. Methods Phys. Res., Sect. B*, 2016, **379**, 219–223.
13 R. Binions, H. Davies, A. Afonja, S. Dungey, D. Lewis, D. E. Williams and I. P. Parkin, *J. Electrochem. Soc.*, 2009, **156**, J46.
14 D. J. Wales, J. Grand, V. P. Ting, R. D. Burke, K. J. Edler, C. R. Bowen, S. Mintova and A. D. Burrows, *Chem. Soc. Rev.*, 2015, **44**, 4290–4321.
15 M. Eddaoudi, D. B. Moler, H. Li, B. Chen, T. M. Reineke, M. O'Keeffe and O. M. Yaghi, *Acc. Chem. Res.*, 2001, **34**, 319–330.
16 H. C. Zhou, J. R. Long and O. M. Yaghi, *Chem. Rev.*, 2012, **112**, 673–674.
17 D. Britt, D. Tranchemontagne and O. M. Yaghi, *Proc. Natl. Acad. Sci. U. S. A.*, 2008, **105**, 11623–11627.
18 I. Stassen, N. Burtch, A. Talin, P. Falcaro, M. Allendorf and R. Ameloot, *Chem. Soc. Rev.*, 2017, **46**, 3185–3241.
19 M. G. Campbell and M. Dinca, *Sensors*, 2017, **17**, 1108–1118.

Table 1 A comparison of the SO_2 sensing properties of the reported materials compared with those of the MOF in the present study

	Sensor materials	Sensing mechanism	Conc. ppm	Temp. °C
Zeolites	Zeolite A[42]	QCM	50	170
	Faujasite[43]	QCM	300	150
Metal oxides	Pt-doped TiO_2 (ref. 44)	Conductivity	5	200
	SnO_2/MgO/V_2O_5 (ref. 45)	Conductivity	1	400
	Pd-doped WO_3 (ref. 46)	Conductivity	1	200
Polymers	Polypyrrole[47]	QCM	10 (vol%)	RT
	Polyaniline[7]	Conductivity	10	RT
Composites	Mn–zeolite Y/PEDOT-PSS[48]	Conductivity	1000	RT
	SnO_2/polyaniline[49]	Conductivity	2	RT
	TiO_2/rGO[a52]	Conductivity	5	RT
MOFs[b]	MFM-300	Capacitance	0.075	RT

[a] Reduced graphene oxide. [b] Current work.

This journal is © The Royal Society of Chemistry 2018

J. Mater. Chem. A, 2018, **6**, 5550–5554 | 5553

20 P. M. Bhatt, Y. Belmabkhout, A. Cadiau, K. Adil, O. Shekhah, A. Shkurenko, L. J. Barbour and M. Eddaoudi, *J. Am. Chem. Soc.*, 2016, **138**, 9301–9307.

21 B. Liu, *J. Mater. Chem.*, 2012, **22**, 10094–10101.

22 F. Y. Yi, D. Chen, M. K. Wu, L. Han and H. L. Jiang, *ChemPlusChem*, 2016, **81**, 675–690.

23 M. G. Campbell and M. Dinca, *Sensors*, 2017, **17**, 1108–1119.

24 C. Sapsanis, H. Omran, V. Chernikova, O. Shekhah, Y. Belmabkhout, U. Buttner, M. Eddaoudi and K. N. Salama, *Sensors*, 2015, **15**, 18153–18166.

25 O. Yassine, O. Shekhah, A. H. Assen, Y. Belmabkhout, K. N. Salama and M. Eddaoudi, *Angew. Chem., Int. Ed.*, 2016, **55**, 15879–15883.

26 M. Savage, Y. Cheng, T. L. Easun, J. E. Eyley, S. P. Argent, M. R. Warren, W. Lewis, C. Murray, C. C. Tang, M. D. Frogley, G. Cinque, J. Sun, S. Rudic, R. T. Murden, M. J. Benham, A. N. Fitch, A. J. Blake, A. J. Ramirez-Cuesta, S. Yang and M. Schroder, *Adv. Mater.*, 2016, **28**, 8705–8711.

27 S. Yang, J. Sun, A. J. Ramirez-Cuesta, S. K. Callear, W. I. David, D. P. Anderson, R. Newby, A. J. Blake, J. E. Parker, C. C. Tang and M. Schroder, *Nat. Chem.*, 2012, **4**, 887–894.

28 S. Yang, L. Liu, J. Sun, K. M. Thomas, A. J. Davies, M. W. George, A. J. Blake, A. H. Hill, A. N. Fitch, C. C. Tang and M. Schroder, *J. Am. Chem. Soc.*, 2013, **135**, 4954–4957.

29 P. K. Thallapally, R. K. Motkuri, C. A. Fernandez, B. P. McGrail and G. S. Behrooz, *Inorg. Chem.*, 2010, **49**, 4909–4915.

30 K. Tan, P. Canepa, Q. Gong, J. Liu, D. H. Johnson, A. Dyevoich, P. K. Thallapally, T. Thonhauser, J. Li and Y. J. Chabal, *Chem. Mater.*, 2013, **25**, 4653–4662.

31 J. B. DeCoste, T. J. Demasky, M. J. Katz, O. K. Farha and J. T. Hupp, *New J. Chem.*, 2015, **39**, 2396–2399.

32 S. Han, Y. Huang, T. Watanabe, S. Nair, K. S. Walton, D. S. Sholl and J. Carson Meredith, *Microporous Mesoporous Mater.*, 2013, **173**, 86–91.

33 C. P. Krap, R. Newby, A. Dhakshinamoorthy, H. Garcia, I. Cebula, T. L. Easun, M. Savage, J. E. Eyley, S. Gao, A. J. Blake, W. Lewis, P. H. Beton, M. R. Warren, D. R. Allan, M. D. Frogley, C. C. Tang, G. Cinque, S. Yang and M. Schroder, *Inorg. Chem.*, 2016, **55**, 1076–1088.

34 O. Shekhah, J. Liu, R. A. Fischer and C. Woll, *Chem. Soc. Rev.*, 2011, **40**, 1081–1106.

35 O. Shekhah and M. Eddaoudi, *Chem. Commun.*, 2013, **49**, 10079–10081.

36 H. C. Streit, M. Adlung, O. Shekhah, X. Stammer, H. K. Arslan, O. Zybaylo, T. Ladnorg, H. Gliemann, M. Franzreb, C. Wöll and C. Wickleder, *ChemPhysChem*, 2012, **13**, 2699–2702.

37 V. Chernikova, O. Shekhah and M. Eddaoudi, *ACS Appl. Mater. Interfaces*, 2016, **8**, 20459–20464.

38 H. Omran and K. N. Salama, *IEEE 3rd International Conference on Smart Instrumentation, Measurement and Applications (ICSIMA)*, 2015, vol. 7559021, pp. 1–4, DOI: 10.1109/ICSIMA.

39 O. Shekhah, H. Wang, S. Kowarik, F. Schreiber, M. Paulus, M. Tolan, C. Sternemann, F. Evers, D. Zacher, R. A. Fischer and C. Woll, *J. Am. Chem. Soc.*, 2007, **129**, 15118–15119.

40 O. Shekhah, C. Busse, A. Bashir, F. Turcu, X. Yin, P. Cyganik, A. Birkner, W. Schuhmann and C. Woll, *Phys. Chem. Chem. Phys.*, 2006, **8**, 3375–3378.

41 E. M. S. Azzam, A. Bashir, O. Shekhah, A. R. E. Alawady, A. Birkner, C. Grunwald and C. Wöll, *Thin Solid Films*, 2009, **518**, 387–391.

42 A. H. Assen, O. Yassine, O. Shekhah, M. Eddaoudi and K. N Salama, *ACS Sens.*, 2017, **2**, 1294–1301.

43 R. Peralta, J. Balmaseda, E. González-Zamora and I. Ibarra, *Inorg. Chem. Front.*, 2015, **2**(12), 1080–1084.

44 I. Sasaki, H. Tsuchiya, M. Nishioka, M. Sadakata and T. Okubo, *Sens. Actuators, B*, 2002, **86**, 26–33.

45 M. Osada, I. Sasaki, M. Nishioka, M. Sadakata and T. Okubo, *Microporous Mesoporous Mater.*, 1998, **23**, 287–294.

46 X. Zhang, J. Tie and J. Zhang, *Sensors*, 2013, **13**, 14764–14776.

47 S. C. Lee, B. W. Hwang, S. J. Lee, H. Y. Choi, S. Y. Kim, S. Y. Jung, D. Ragupathy, D. D. Lee and J. C. Kim, *Sens. Actuators, B*, 2011, **160**, 1328–1334.

48 M. Stankova, X. Vilanova, J. Calderer, E. Llobet, P. Ivanov, I. Gràcia, C. Cané and X. Correig, *Sens. Actuators, B*, 2004, **102**, 219–225.

49 V. Syritski, J. Reut, A. Öpik and K. Idla, *Synth. Met.*, 1999, **102**, 1326–1327.

50 P. Chanthaanont and A. Sirivat, *Adv. Polym. Technol.*, 2013, **32**, 21367.

51 C. A. Betty, S. Choudhury and S. Arora, *Sens. Actuators, B*, 2015, **220**, 288–294.

52 D. Zhang, J. Liu, C. Jiang, P. Li and Y. e. Sun, *Sens. Actuators, B*, 2017, **245**, 560–567.

53 S. Park, C. Park and H. Yoon, *Polymers*, 2017, **9**, 155.

5554 | *J. Mater. Chem. A*, 2018, **6**, 5550–5554

This journal is © The Royal Society of Chemistry 2018